Experimental Animals
Exp. Anim. 73(1), 1–10, 2024

Original

Disruption of testis-enriched cytochrome c oxidase subunit COX6B2 but not COX8C leads to subfertility

Keisuke SHIMADA[1)], Yonggang LU[1)] and Masahito IKAWA[1,2)]

[1)]*Department of Experimental Genome Research, Research Institute for Microbial Diseases, Osaka University, 3-1 Yamada-oka, Suita, Osaka 565-0871, Japan*
[2)]*Laboratory of Reproductive Systems Biology, Center for Experimental Medicine and Systems Biology, The Institute of Medical Science, The University of Tokyo, 4-6-1 Shirokanedai, Minato-ku, Tokyo 108-8639, Japan*

Abstract: Mammalian sperm flagellum contains the midpiece characterized by a mitochondrial sheath that packs tightly around the axoneme and outer dense fibers. Mitochondria are known as the “powerhouse” of the cell, and produce ATP through the tricarboxylic acid (TCA) cycle and oxidative phosphorylation (OXPHOS). However, the contribution of the TCA cycle and OXPHOS to sperm motility and male fertility is less clear. Cytochrome c oxidase (COX) is an oligomeric complex localized within the mitochondrial inner membrane, and the terminal enzyme of the mitochondrial electron transport chain in eukaryotes. Both COX6B2 and COX8C are testis-enriched COX subunits whose functions in vivo are poorly studied. Here, we generated *Cox6b2* and *Cox8c* knockout (KO) mice using the CRISPR/Cas9 system. We examined their fertility and sperm mitochondrial function to determine the significance of testis-enriched COX subunits in male fertility. The mating test revealed that disrupting COX6B2 induces male subfertility, while disrupting COX8C does not affect male fertility. *Cox6b2* KO spermatozoa showed low sperm motility, but mitochondrial function was normal according to oxygen consumption rates. Therefore, low sperm motility seems to cause subfertility in *Cox6b2* KO male mice. These results also indicate that testis-enriched COX, COX6B2 and COX8C, are not essential for OXPHOS in mouse spermatozoa.
Key words: CRISPR/Cas9, cytochrome c oxidase subunit, mitochondria, sperm motility, subfertility

Introduction

A spermatozoon consists of a head and a flagellum that provides the locomotive force required for delivery of the haploid male genome to the oocyte. The mammalian sperm flagellum is divided into a midpiece, principal piece, and end piece region, with the midpiece characterized by the mitochondrial sheath that packs tightly around the axoneme and the outer dense fibers [1]. There are numerous reports that an abnormal mitochondrial sheath structure results in decreased sperm motility, which in turn results in male infertility [2–8]. Therefore, it is no wonder that appropriate mitochondrial sheath formation is important for male fertility. In addition, mitochondria as the “powerhouse” of the cell are the location of two sources of ATP production, the tricarboxylic acid (TCA) cycle and oxidative phosphorylation (OXPHOS), after glycolysis in the cytosol [9]. Sperm-specific glycolytic enzyme (GAPDS and PGK2) disruptions lead to low sperm motility, ATP production, and male infertility without morphological defects in spermatozoa [10, 11]. Therefore, ATP production via glycolysis is necessary for male fertility, but the contribution of the TCA cycle and OXPHOS is less clear. Oxygen consumption rate (OCR) is an indicator of mitochondrial respiration [12]. Several reports show low ATP and OCR levels or OXPHOS-related activity in some gene-manipulated mouse spermatozoa, as well as

(Received 23 April 2023 / Accepted 4 July 2023 / Published online in J-STAGE 10 July 2023)
Corresponding authors: K. Shimada. email: shimada-k@biken.osaka-u.ac.jp
M. Ikawa. email: ikawa@biken.osaka-u.ac.jp
Supplementary Tables: refer to J-STAGE: https://www.jstage.jst.go.jp/browse/expanim

This is an open-access article distributed under the terms of the Creative Commons Attribution Non-Commercial No Derivatives (by-nc-nd) License <http://creativecommons.org/licenses/by-nc-nd/4.0/>.
©2024 Japanese Association for Laboratory Animal Science

low sperm motility and male infertility, but these spermatozoa also exhibit morphological abnormalities [5, 13]. Therefore, direct evidence of the importance of ATP synthesis via mitochondria in male fertility is less clear.

Cytochrome c oxidase (COX) or complex IV is an oligomeric complex localized within the mitochondrial inner membrane [14], and the terminal enzyme of the mitochondrial electron transport chain (ETC) in eukaryotes [15]. COX catalyzes electron transfer from cytochrome c to molecular oxygen, reducing it to water. The reaction is accompanied by vectorial transport (pumping) of four protons across the membrane [16]. The energy accumulated in the proton gradient over the inner membrane is utilized for OXPHOS, which synthesize ATP by an ATP synthase [17]. The mammalian COX has 13 subunits, and it is known that certain subunits show tissue-specific expression [18]. COX6B2, COX7B2, and COX8C are testis-enriched COX subunits [18], and overexpressed COX6B2 and COX8C localize to mitochondria in cultured cells [19, 20]. A previous study generated knockout (KO) mice targeting testis-enriched COX subunit genes, *Cox7b2* and *Cox8c*, and confirmed the effect on male germ cells. This previous study revealed that *Cox7b2* KO male mice produced poorly motile infertile spermatozoa, while *Cox8c* KO mice produced functional spermatozoa [21]. However, *Cox6b2* KO mice have not yet been reported. Additionally, the previous paper did not demonstrate a detailed analysis of *Cox8c* KO mice. Here, we generated *Cox6b2* and *Cox8c* KO mice, respectively using the CRISPR/Cas9 system, and examined their fertility. We also assessed the mitochondrial function of their spermatozoa to determine the significance of the testis-enriched COX subunit in male fertility.

Materials and Methods

Animals

All animal experiments were approved by the Animal Care and Use Committees of the Research Institute for Microbial Diseases, Osaka University (Osaka, Japan) (Approval number: Biken-AP-H30-01-1) in accordance with the animal testing guidelines and regulations. Animals were housed in a temperature-controlled environment with 12 h light cycles and free access to food and water. B6D2F1 (C57BL/6 × DBA2), C57BL/6N or ICR mice were used as embryo donors, RNA extraction or foster mothers, respectively. These mice were purchased from CLEA Japan, Inc. (Tokyo, Japan) or Japan SLC, Inc. (Shizuoka, Japan). B6D2-Tg (CAG/Su9-DsRed2, Acr3-EGFP) RBGS002Osb (RBGS, Red Body Green Sperm) mice [22] were used for observing sperm mitochondria.

RT-PCR

RT-PCR was conducted as previously described [23]. Total RNA was prepared from multiple adult tissues of C57BL/6N mice using TRIzol (ThermoFisher Scientific, Waltham, MA, USA). The obtained total RNA was reverse transcribed to cDNA with the SuperScript IV Reverse Transcriptase (ThermoFisher Scientific) using an oligo (dT) primer. PCR was then performed using 10 ng cDNA with the primers listed in Supplementary Table 1.

Generation of knockout mice using the CRISPR/Cas9 system

Cox6b2 and *Cox8c* KO mice were generated by electroporation described previously [24]. The cleavage target sites were designed in the first and last exons to remove almost the whole coding sequence for each gene (Figs. 1B and C). The crRNA sequences for generating *Cox6b2* KO mice were 5′- AGCCAGCCAATCCGGCCTGA −3′ and 5′- CTAGGGGTTGATGACGCCAG −3′ and those for *Cox8c* were 5′- GGTGGCCAGGCTTCGAGAAC −3′ and 5′- TTATAGGACTAACTCGTCAG −3′. Synthesized crRNAs (Merck, Darmstadt, Germany), tracrRNA (Merck) and CAS9 protein (Thermo Fisher Scientific) were incubated to make the CAS9 ribonucleoprotein (RNP) complex. The obtained RNP complex was electroporated into fertilized oocytes using a NEPA21 electroporator (NEPA GENE, Chiba, Japan). For generating *Cox6b2* KO mice, of the 100 fertilized eggs that had been electroporated with RNP, 94 eggs were transplanted into the oviducts of pseudopregnant females. A total of 21 mice were born, and 4 pups possessed mutations in the *Cox6b2* gene. For generating *Cox8c* KO mice, of the 76 fertilized eggs that had been electroporated with RNP, 71 eggs were transplanted into the oviducts of pseudopregnant females. A total of 15 mice born, and 12 pups possessed mutations in the *Cox8c* gene. Genotyping was conducted by PCR and Sanger sequencing. The primers and PCR conditions for genotyping are listed in Supplementary Table 1.

Fertility analysis

Sexually mature wild-type (WT) or KO male mice were individually housed with three 6-week-old female B6D2F1 mice for 8 weeks. Male mice were removed after an 8-week mating period and females were maintained for an additional 3 weeks to count the final offspring. The number of pups and copulation plugs were counted every weekday morning.

Morphological and histological analysis of testis

Male mice (11–12 weeks old) were euthanized and

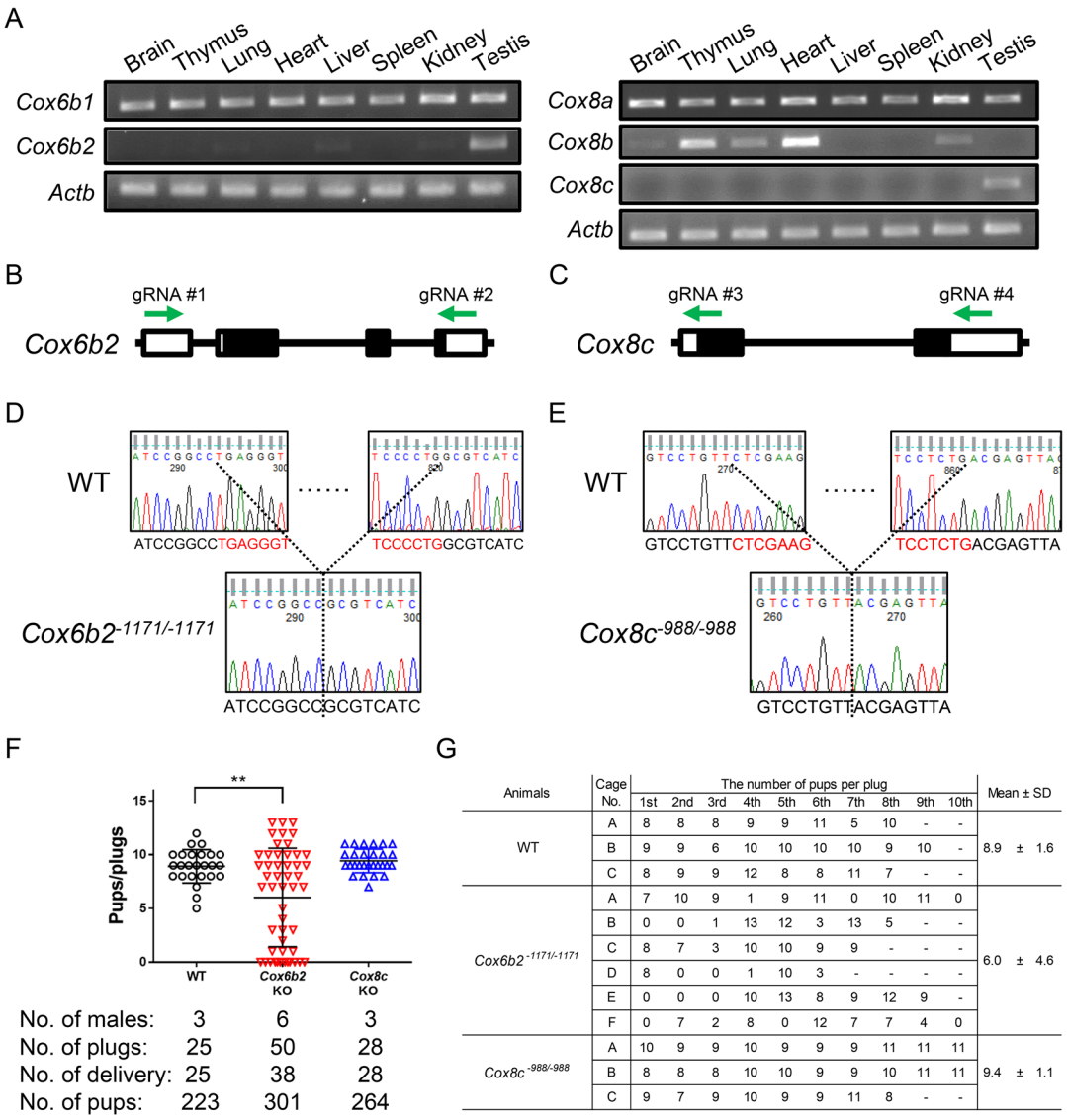

G

Animals	Cage No.	The number of pups per plug										Mean ± SD
		1st	2nd	3rd	4th	5th	6th	7th	8th	9th	10th	
WT	A	8	8	8	9	9	11	5	10	-	-	8.9 ± 1.6
	B	9	9	6	10	10	10	10	9	10	-	
	C	8	9	9	12	8	8	11	7	-	-	
Cox6b2$^{-1171/-1171}$	A	7	10	9	1	9	11	0	10	11	0	6.0 ± 4.6
	B	0	0	1	13	12	3	13	5	-	-	
	C	8	7	3	10	10	9	9	-	-	-	
	D	8	0	0	1	10	3	-	-	-	-	
	E	0	0	0	10	13	8	9	12	9	-	
	F	0	7	2	8	0	12	7	7	4	0	
Cox8c$^{-988/-988}$	A	10	9	9	10	9	9	9	11	11	11	9.4 ± 1.1
	B	8	8	8	10	10	9	9	10	11	11	
	C	9	7	9	10	9	9	11	8	-	-	

Fig. 1. *Cox6b2*-disrupted male mice are subfertile. (A) The expression of mouse *Cox6b* and *Cox8* family genes was examined by RT-PCR using RNA isolated from various organs. Both *Cox6b2* and *Cox8c* show testis-enriched expression. *Actb* was used as a loading control. (B, C) KO strategy for generating *Cox6b2* (B) and *Cox8c* (C) KO mice. Panels show a diagram of each gene. Two gRNAs (green arrows) were designed to target the first and last exons. (D, E) The DNA sequence of the control and KO mouse lines in the *Cox6b2* (D) and *Cox8c* (E) genes. A *Cox6b2* KO mouse line that has 1,171-bp deletion and *Cox8c* KO mouse line that has 988-bp deletion were generated in the present study. (F, G) The graph (F) and table (G) indicate the number of litters born per plug detected. Males for each WT, *Cox6b2* and *Cox8c* KO were mated with three WT females per male.

testes were dissected. After measuring the testicular weight, testes were fixed with Bouin's fixative (Polysciences, Warrington, PA, USA). Fixed testes were embedded in paraffin, sectioned, rehydrated, and treated with 1% periodic acid for 10 min, followed by treatment with Schiff's reagent (Fujifilm Wako Pure Chemical, Osaka, Japan) for 20 min. The sections were stained with Mayer's haematoxylin solution (Fujifilm Wako Pure Chemical) prior to imaging and observed using an Olympus BX53 microscope (Olympus, Tokyo, Japan).

Immunofluorescence analysis of cultured cells

Immunofluorescence analysis of cultured cells was performed as previously described with slight modification [7]. COS-7 cells (1.5×10^5 cells) were seeded on coverslips (Matsunami Glass, Osaka, Japan) in a 6-well plate. After 6–8 h, expressing vectors were transiently transfected into COS-7 cells using PEI MAX (Polyscience, Warrington, PA, USA). After 40 h, cells were washed with PBS, fixed by 4% PFA and permeabilized with 0.5% Triton X-100. Cells were blocked with 3% BSA and immunostained. The cells were incubated with primary antibodies overnight at 4°C. After washing three

times, the cells were incubated with AlexaFluor-conjugated secondary antibodies for 2 h at room temperature. The cells were then washed three times and stained with Hoechst 33342 (ThermoFisher Scientific) for visualizing nuclei. The mitochondria marker TOM20 was used for visualizing mitochondria. After washing three times, the cells were mounted on MAS coated glass slides (Matsunami Glass) with Immu-Mount (ThermoFisher Scientific). Microscopic images were obtained using a Nikon Eclipse Ti microscope connected to a C2 confocal module (Nikon, Tokyo, Japan). Fluorescent images were false-colored and cropped using ImageJ software (version 2.0.0, NIH, Bethesda, MD, USA). The antibodies used in this study are listed in Supplementary Table 2.

Morphological analysis of spermatozoa

Spermatozoa from male mice with the RBGS transgene were used for this analysis. Spermatozoa were collected from the cauda epididymis, and suspended in Toyoda, Yokoyama, and Hoshi (TYH) medium [25] with 10 μg/ml of Hoechst 33342. After a 10 min incubation at 37°C under 5% CO_2, a sperm suspension was mounted on MAS coated glass slide, and a cover slip was added. Immunofluorescence and sperm shape were observed using an Olympus BX53 microscope.

Oxygen consumption rate of spermatozoa

Measurement of OCR of the spermatozoa was performed using a Seahorse XFp analyzer (Seahorse Bioscience, North Billerica, MA, USA) as previously described [8] with slight modifications. Mature spermatozoa were collected from the cauda epididymis in flushing holding medium (FHM, non-capacitation medium) [26]. The spermatozoa (2.5×10^6 per well) were transferred to an 8-well plate that had been coated with concanavalin A (Fujifilm Wako Pure Chemical) at 0.5 mg/ml (20 μl per well), and the plate was centrifuged at 1,200 × g for 2 min. The OCR was measured using a Seahorse XFp Cell Mito Stress Test Kit. The spermatozoa were exposed to 1.5 μM oligomycin for 19.8 min, to 2.0 μM FCCP for 19.8 min, and then to rotenone and antimycin (1.0 μM each) for 19.8 min. Spermatozoa were collected from each well for measurement of protein content and normalization of OCR values. Basal respiration was the OCR before drug injection. ATP production was calculated as the difference between the basal OCR and the OCR after oligomycin injection. Proton leak was the OCR after oligomycin injection. Maximal respiration was the OCR after FCCP injection. Spare capacity is calculated as the difference between OCR after FCCP injection and basal respiration [27].

Sperm motility analysis

Sperm motility analysis was performed as previously described [28]. Cauda epididymal spermatozoa were suspended and incubated in TYH medium that can induce sperm capacitation [25]. Spermatozoa were loaded onto prewarmed 100 μm deep Leja counting chamber slides (Leja, Nieuw-Vennep, The Netherlands) for analysis. Sperm motility was then measured using the CEROS II sperm analysis system (software version 1.5; Hamilton Thorne Biosciences, Beverly, MA, USA). The motility of epididymal spermatozoa was recorded after 10 min and 2 h of incubation in TYH medium.

For waveform tracing, spermatozoa were observed with an Olympus BX53 microscope equipped with a high-speed camera (HAS-L1, Ditect, Tokyo, Japan). The motility was videotaped at 200 frames per second and analyzed for waveforms using the sperm motion analyzing software (BohBohsoft, Tokyo, Japan) [29].

Immunoblot analysis

Immunoblot analysis was performed as previously described [30]. Spermatozoa collected from the cauda epididymis were incubated in TYH medium for 10 min or 2 h. Spermatozoa were then collected in PBS and centrifugated at 2,000 g for 2 min at room temperature. The collected spermatozoa were resuspended in 2% sample buffer, boiled for 5 min, centrifuged at 15,000 *g* for 10 min, and collected supernatant. Samples were subjected to SDS-PAGE followed by western blotting. After blocking with 5% skim milk, blots were incubated with primary antibodies overnight at 4°C and then incubated with secondary antibodies conjugated to horseradish peroxidase for 2 h at room temperature. The antibodies used in this study and their dilution conditions are listed in Supplementary Table 2.

Statistical analysis

Statistical analyses were performed using a two-tailed unpaired *t*-test (n≥3) by GraphPad Prism 6 (GraphPad, San Diego, CA, USA). *P* values less than 0.05 were considered significant. Data represent the means and error bars indicate SD.

Mouse resources

KO mouse lines used in this study were deposited and available through either the Riken BioResource Center (Riken BRC; Tsukuba, Japan) or the Center for Animal Resources and Development, Kumamoto University (CARD; Kumamoto, Japan). The *Cox6b2* KO mouse line was deposited under the name B6D2-*Cox6b2*^{em1Osb}, and the stock ID number is 11457 (Riken BRC) or 3101 (CARD), respectively. The *Cox8c* KO mouse line was

deposited under the name B6D2-*Cox8c*^{em1Osb}, and the stock ID number is 11017 (Riken BRC) or 2924 (CARD), respectively.

Results

Generation of testis-enriched COX subunit gene KO mice

To confirm testis-enriched expression of *Cox6b2* and *Cox8c* [19, 21, 31], we performed RT-PCR for *Cox6b* and *Cox8* families using multiple tissues from adult mice. RT-PCR revealed that both *Cox6b2* and *Cox8c* showed testis-enriched expression (Fig. 1A), consistent with previous studies and database (https://orit.research.bcm.edu/MRGDv2) [32]. In contrast, *Cox6b1* and *Cox8a* demonstrate ubiquitous expression, with *Cox8b* expressed in thymus, lung, heart and kidney. We then generated testis-enriched COX subunit gene KO mice using the CRISPR/Cas9 system to clarify the role of each gene in the testis. Guide RNAs that target upstream of the start codon and downstream of the stop codon were used (Figs. 1B and C). Mutant mouse lines that possessed a 1,171 bp deletion in the *Cox6b2* gene and a 988 bp deletion in the *Cox8c* gene, respectively were obtained and used for this study (Figs. 1D and E). Both *Cox6b2* and *Cox8c* KO mice are viable and show no overt developmental or behavioral abnormalities. To test the fertility of the mice, individual (WT or KO) male mice were housed with WT females for 2 months. Although *Cox8c* KO male mice produced a comparable number of pups as WT male mice, the average litter size of *Cox6b2* KO male mice was significantly lower than WT males (Fig. 1F). Upon examination of the number of pups produced per plug, we observed that *Cox6b2* KO male mice sometimes failed to produce pups or produced only a few pups after mating (Fig. 1G). These results indicate that the disruption of *Cox6b2* induces subfertility in male mice, but *Cox8c* is dispensable for male fertility. We also checked the fertility of both *Cox6b2* and *Cox8c* KO female mice, but there were no problems with their fertility. Average litter size of *Cox6b2* and *Cox8c* KO female mice were 7.2 ± 1.6 and 6.7 ± 2.1, respectively (mean ± SD, n>14).

Cox6b2 KO spermatozoa show low motility

We then examined the testis weight and the histology of the testis. Both *Cox6b2* and *Cox8c* KO male mice have no problems with their gross appearance (Figs. 2A and D), testis weight (Figs. 2B and E) and histology (Figs. 2C and F). Since COX is embedded in the mitochondrial inner membrane [33], both COX6B2 and COX8C are expected to function in sperm mitochondria. To examine their subcellular localization, we transiently expressed epitope-tagged COX6B2 or COX8C proteins in COS-7 cells. Both COX6B2 and COX8C co-localized with the mitochondrial marker TOM20; overexpression of either protein did not alter the morphology of mitochondria (Fig. 3A). We then observed mitochondrial sheath structures in both KO mouse lines, but no morphological abnormalities in spermatozoa were observed (Fig. 3B). COX is a terminal enzyme of the respiratory chain and a key regulatory site of the mitochondrial OXPHOS system [34]. Therefore, we measured the oxygen consumption rate (OCR), which is an indicator of mitochondrial activity of OXPHOS [35], in KO spermatozoa under non-capacitation condition. However, we could not find any difference in the OCR related to basal respiration, ATP production, proton leak, maximal respiration and spare capacity between WT, *Cox6b2* and *Cox8c* KO spermatozoa (Figs. 3C and D).

We then checked the motility of the spermatozoa using the computer-assisted sperm analysis (CASA) system. While sperm motility and progressive sperm rate were unchanged at 10 min incubation, they were significantly lower in *Cox6b2* KO spermatozoa than those of control at 120 min incubation (Figs. 4A and B). In addition, we found that *Cox6b2* KO spermatozoa had lower motility in terms of VAP (average-path velocity) at 120-min, VCL (curvilinear velocity) at 10-min, and VSL (straight-line velocity) at 120-min incubation (Figs. 4C–E). On the other hand, there were no significant changes in sperm motility between control and *Cox8c* KO spermatozoa (Figs. 4F–J). To check whether spermatozoa were capacitated in 120 min incubation, we analyzed the phosphorylation status of tyrosine residues, a hallmark of the capacitation process [36]. Then we found that tyrosine was phosphorylated in both control and KO spermatozoa after 120 min of incubation (Fig. 4K). This result indicates that control, *Cox6b2* and *Cox8c* KO spermatozoa undergo adequate capacitation. To further evaluate sperm motility, we traced the flagellar waveform of the spermatozoa, but there were no changes between WT and both KO mice (Fig. 4L). Based on these results, it appears that lower sperm motility is responsible for the subfertility in *Cox6b2* KO male mice.

Discussion

Both *Cox6b2* and *Cox8c* show testis-enriched expression (Fig. 1A), and encode proteins localized to mitochondria in cultured cells (Fig. 3A). As COX is known as the terminal enzyme of the mitochondrial ETC [15], we expected that testis-enriched COX subunit gene-disrupted mice would have abnormal mitochondrial

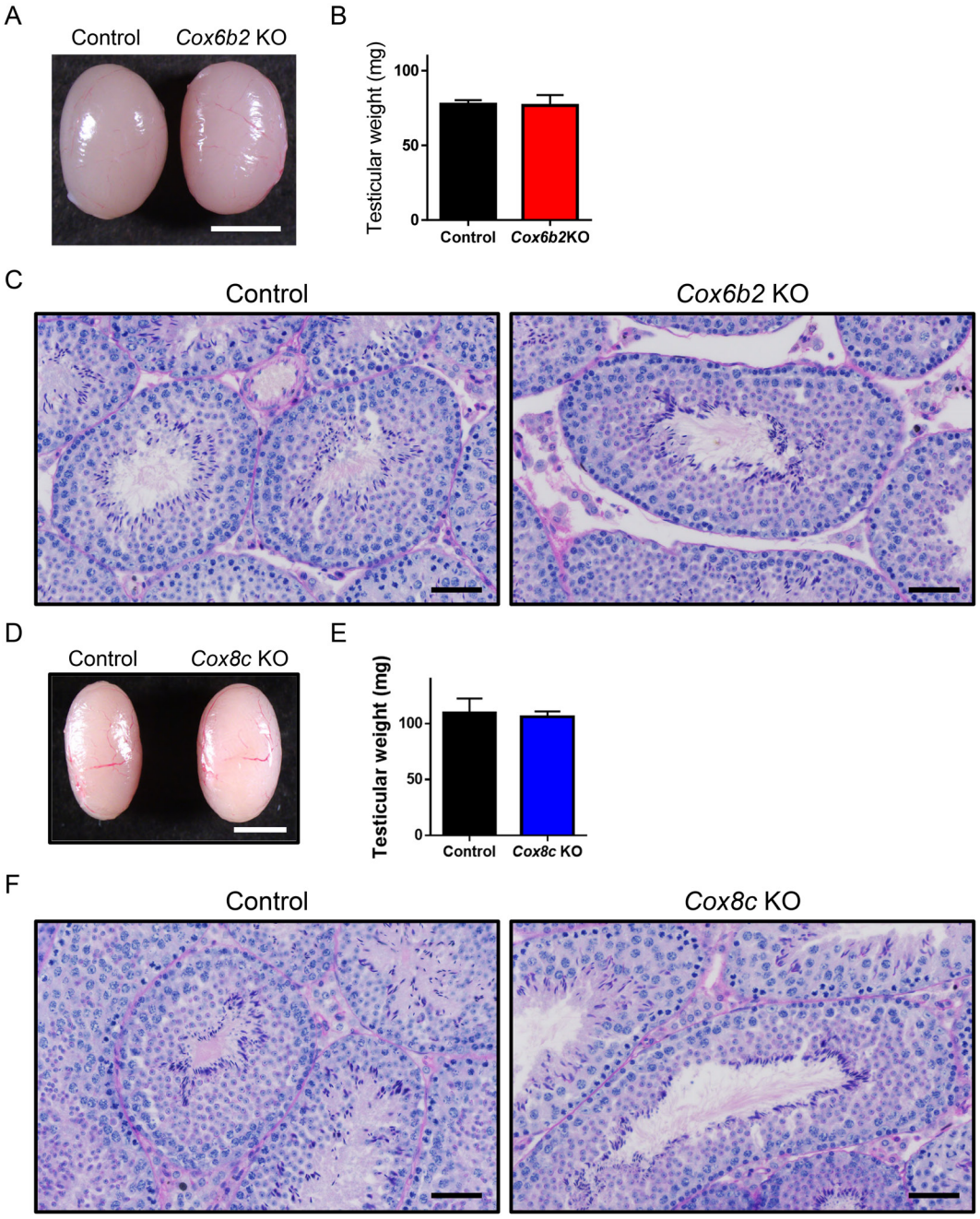

Fig. 2. No abnormalities were detected in both *Cox6b2* and *Cox8c* KO mouse testis. (A) Gross morphology of control and *Cox6b2* KO testes. Scale bars: 3.0 mm. (B) Testis weight of control and *Cox6b2* KO mice (*N*=4). Average weight of testis in control=77.5 ± 2.8 mg; *Cox6b2* KO=76.7 ± 7.0 mg. *P*=0.7712, Student's *t*-test; error bars represent SD. (C) PAS staining of testis samples from control and *Cox6b2* KO male mice. Scale bars: 50 μm. (D) Gross morphology of control and *Cox8c* KO testes. Scale bars: 3.0 mm. (E) Testis weight of control and *Cox8c* KO mice (*N*=4). Average weight of testis was control=109.5 ± 13.0 mg; *Cox8c* KO=106.1 ± 4.8 mg. *P*=0.1718, Student's *t*-test; error bars represent SD. (F) PAS staining of testis samples from control and *Cox8c* KO male mice. Scale bars: 50 μm.

function in spermatozoa. However, neither *Cox6b2* nor *Cox8c* KO spermatozoa exhibited impaired mitochondrial function under non-capacitation condition (Figs. 3C and D). Because *Cox6b1* and *Cox8a*, are also expressed in the testis (Fig. 1A), those encode proteins may compensate testis-enriched COX subunit proteins. Previous study confirmed that COX6B2 enhanced complex IV activity, resulting in an increase in mitochondrial OXPHOS, and its depletion impaired mitochondrial ETC function [37]. In addition, several studies have shown that COX6B2 is activated in cancer cells, thereby increasing OXPHOS [37, 38]. Therefore, it is reasonable to assume that the family protein compensates for the function of testis-enriched proteins in KO spermatozoa.

 doi: 10.1538/expanim.23-0055

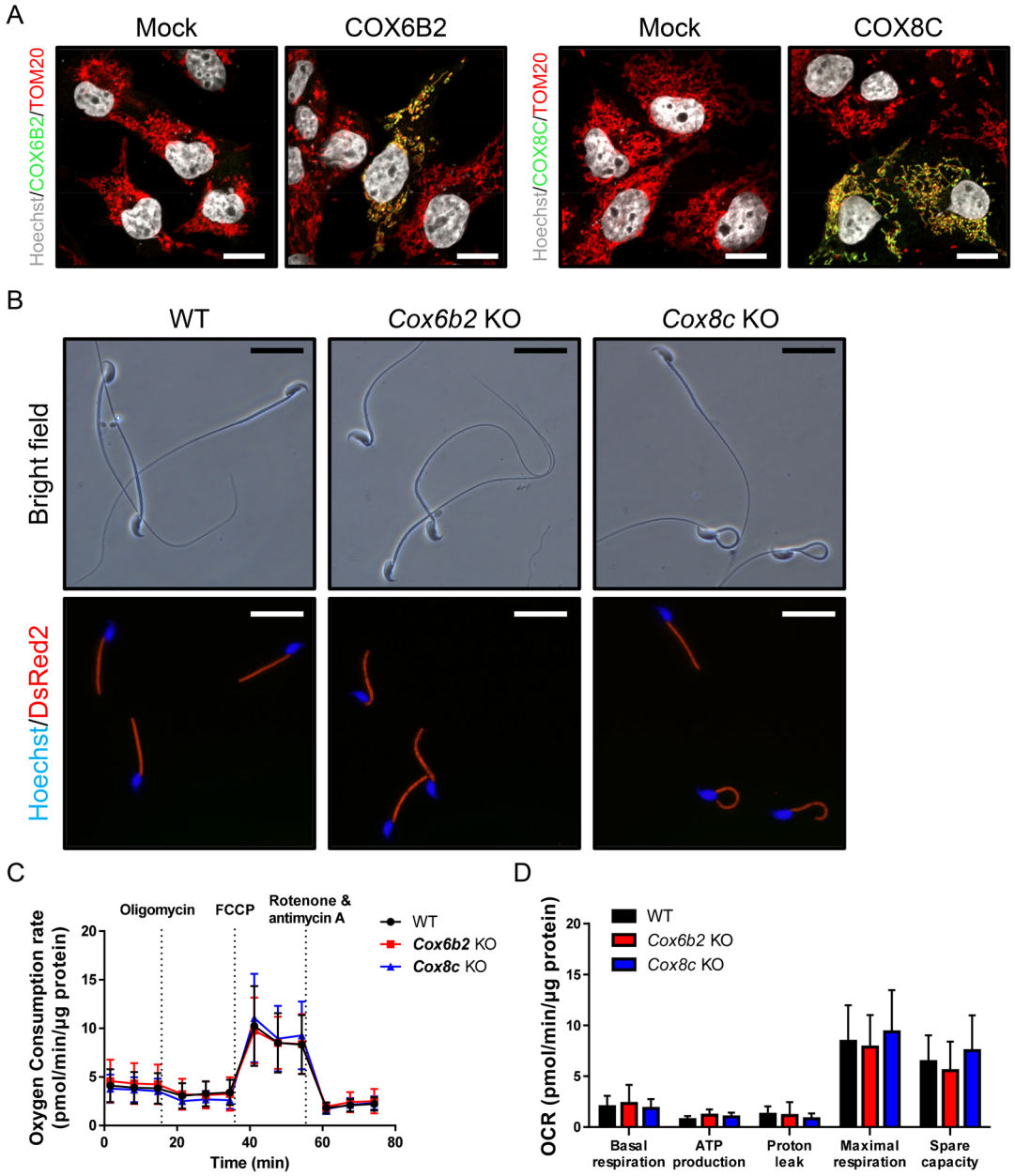

Fig. 3. Both *Cox6b2* and *Cox8c* KO spermatozoa have no abnormalities in mitochondrial sheath formation and mitochondrial function. (A) Fluorescence images after transient expression of testis-enriched COX subunit genes in COS-7 cells. COS-7 cells were transiently expressed with mock vector, 8xHis- and 1D4-tagged COX6B2 expression vector or 3xHA-tagged COX8C expression vector, and stained with 1D4 or HA (green), TOM20 (red) and Hoechst 33342 (white) to visualize COX subunit, mitochondria and nuclei, respectively. Scale bars: 20 μm. (B) Sperm morphology of WT, *Cox6b2*, and *Cox8c* KO mice in the RBGS background, which express mitochondria-targeted DsRed2 (red). Nuclei were stained with Hoechst 33342 (blue). Scale bars: 20 μm. (C, D) Oxygen consumption rate (OCR) traces for spermatozoa collected from the cauda epididymis of WT, *Cox6b2*, and *Cox8c* KO mice (C), as well as quantification of basal respiration, ATP production, proton leak, maximal respiration, and spare capacity (D). Error bars represent SD, N=4.

Due to the lack of suitable antibodies against COX6B2 and COX8C, we could not determine the localization of these testis-enriched COX subunits or their interactome *in vivo*. Our data (Fig. 3A) and previous studies [19, 20] demonstrated that COX6B2 and COX8C co-localized to mitochondria in cultured cells. There is, however, no direct evidence that COX6B2 and COX8C are localized to the inner membrane of mitochondria in male germ cells.

The mating test revealed that disrupting COX6B2 induces male subfertility, while disrupting COX8C does not affect male fertility (Figs. 1F and G). Male mice with a *Cox6b2*-disruption are capable of producing pups, however occasionally they are unable to produce pups

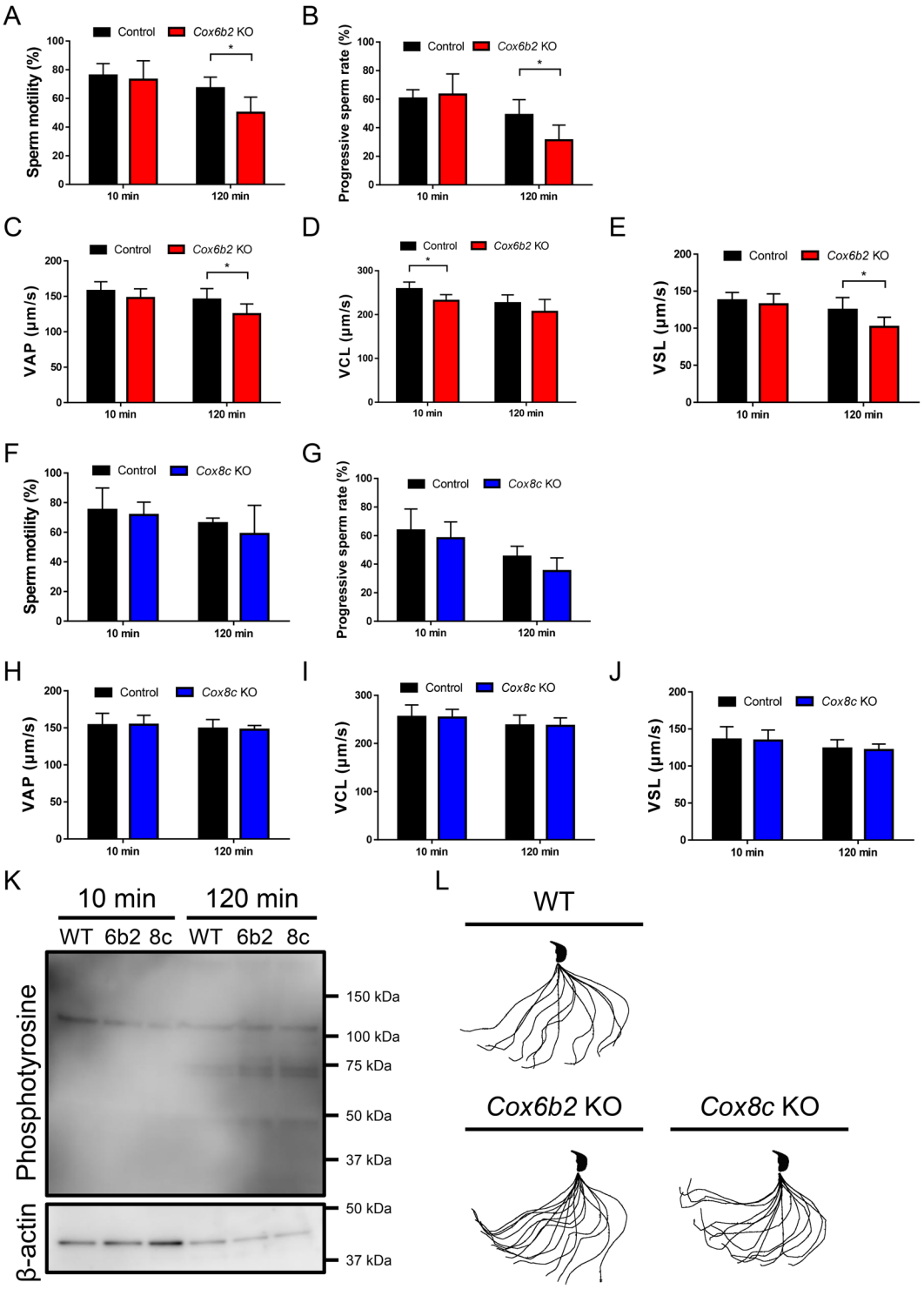

Fig. 4. *Cox6b2* KO spermatozoa show low motility, but not *Cox8c* KO. (A, B) Sperm motility (A) and progressive sperm rate (B) from control and *Cox6b2* KO mice. (C–E) The means of VAP (C), VCL (D) and VSL (E) from control and *Cox6b2* KO mice. (F, G) Sperm motility (F) and progressive sperm rate (G) from control and *Cox8c* KO mice. (H–J) The means of VAP (H), VCL (I), and VSL (J) from control and *Cox8c* KO mice. **P*<0.05, Student's *t*-test; error bars represent SD (*N*=6). (K) Phosphorylation status of tyrosine residues of sperm proteins. β-actin was used as a loading control. (L) Flagellar waveforms were analyzed 10 min after incubation. Single frames throughout one beating cycle were superimposed.

even after successful copulation with females (Fig. 1G). *Cox6b2* KO spermatozoa exhibit no abnormalities in sperm morphology (Fig. 3B) or mitochondrial function under non-capacitation condition (Figs. 3C and D), but show low sperm motility (Figs. 4A–E) without any abnormalities in capacitation (Fig. 4K) and flagellar wave-

 doi: 10.1538/expanim.23-0055

form (Fig. 4L). Therefore, low sperm motility seems to cause subfertility in *Cox6b2* KO male mice. However, the cause of reduced sperm motility remains unknown. Our present study on testis-enriched COX subunit gene-disrupted male mice does not support the necessity or unnecessity of OXPHOS in sperm functionality. We hope further studies will reveal the role of ATP production via the mitochondrial TCA cycle and OXPHOS in male reproduction.

Author Contributions

K. Shimada and M. Ikawa designed the research and wrote the paper; K. Shimada and Y. Lu performed the research and analyzed the data.

Acknowledgment

We thank Kotone Kawamura, Eri Hosoyamada, Mei Koyama, and the NPO for Biotechnology Research and Development for technical support. We also appreciate Dr. Julio M. Castaneda for critical reading of this manuscript. We also thank the Department of Experimental Genome Research and the Animal Resource Center for Infectious Diseases for creating a suitable environment for the experiments.

This work was supported by the Japan Society for the Promotion of Science (JSPS) KAKENHI grants (JP20K16107 to K.S., JP22K15103 to Y.L., and JP19H05750, JP21H04753, JP21H05033 to M.I.); Japan Agency for Medical Research and Development (AMED) grant JP21gm5010001 to M.I.; Takeda Science Foundation grants to K.S.; Senri Life Science Foundation grant to K.S.; the Eunice Kennedy Shriver National Institute of Child Health and Human Development (P01HD087157 and R01HD088412 to M.I); the Bill & Melinda Gates Foundation (Grand Challenges Explorations grant INV-001902 to M.I.).

References

1. Fawcett DW. The mammalian spermatozoon. Dev Biol. 1975; 44: 394–436. [Medline] [CrossRef]
2. Schneider M, Förster H, Boersma A, Seiler A, Wehnes H, Sinowatz F, et al. Mitochondrial glutathione peroxidase 4 disruption causes male infertility. FASEB J. 2009; 23: 3233–3242. [Medline] [CrossRef]
3. Johnson AR, Craciunescu CN, Guo Z, Teng YW, Thresher RJ, Blusztajn JK, et al. Deletion of murine choline dehydrogenase results in diminished sperm motility. FASEB J. 2010; 24: 2752–2761. [Medline] [CrossRef]
4. Baba T, Kashiwagi Y, Arimitsu N, Kogure T, Edo A, Maruyama T, et al. Phosphatidic acid (PA)-preferring phospholipase A1 regulates mitochondrial dynamics. J Biol Chem. 2014; 289: 11497–11511. [Medline] [CrossRef]
5. Mi Y, Shi Z, Li J. Spata19 is critical for sperm mitochondrial function and male fertility. Mol Reprod Dev. 2015; 82: 907–913. [Medline] [CrossRef]
6. Shimada K, Kato H, Miyata H, Ikawa M. Glycerol kinase 2 is essential for proper arrangement of crescent-like mitochondria to form the mitochondrial sheath during mouse spermatogenesis. J Reprod Dev. 2019; 65: 155–162. [Medline] [CrossRef]
7. Shimada K, Park S, Miyata H, Yu Z, Morohoshi A, Oura S, et al. ARMC12 regulates spatiotemporal mitochondrial dynamics during spermiogenesis and is required for male fertility. Proc Natl Acad Sci USA. 2021; 118: e2018355118. [Medline] [CrossRef]
8. Mise S, Matsumoto A, Shimada K, Hosaka T, Takahashi M, Ichihara K, et al. Kastor and Polluks polypeptides encoded by a single gene locus cooperatively regulate VDAC and spermatogenesis. Nat Commun. 2022; 13: 1071. [Medline] [CrossRef]
9. Bonora M, Patergnani S, Rimessi A, De Marchi E, Suski JM, Bononi A, et al. ATP synthesis and storage. Purinergic Signal. 2012; 8: 343–357. [Medline] [CrossRef]
10. Miki K, Qu W, Goulding EH, Willis WD, Bunch DO, Strader LF, et al. Glyceraldehyde 3-phosphate dehydrogenase-S, a sperm-specific glycolytic enzyme, is required for sperm motility and male fertility. Proc Natl Acad Sci USA. 2004; 101: 16501–16506. [Medline] [CrossRef]
11. Danshina PV, Geyer CB, Dai Q, Goulding EH, Willis WD, Kitto GB, et al. Phosphoglycerate kinase 2 (PGK2) is essential for sperm function and male fertility in mice. Biol Reprod. 2010; 82: 136–145. [Medline] [CrossRef]
12. Ferrick DA, Neilson A, Beeson C. Advances in measuring cellular bioenergetics using extracellular flux. Drug Discov Today. 2008; 13: 268–274. [Medline] [CrossRef]
13. Kuang W, Zhang J, Lan Z, Deepak RNVK, Liu C, Ma Z, et al. SLC22A14 is a mitochondrial riboflavin transporter required for sperm oxidative phosphorylation and male fertility. Cell Rep. 2021; 35: 109025. [Medline] [CrossRef]
14. Carr HS, Winge DR. Assembly of cytochrome c oxidase within the mitochondrion. Acc Chem Res. 2003; 36: 309–316. [Medline] [CrossRef]
15. Čunátová K, Reguera DP, Houštěk J, Mráček T, Pecina P. Role of cytochrome c oxidase nuclear-encoded subunits in health and disease. Physiol Res. 2020; 69: 947–965. [Medline] [CrossRef]
16. Michel H. The mechanism of proton pumping by cytochrome c oxidasex127e [comments]. Proc Natl Acad Sci USA. 1998; 95: 12819–12824. [Medline] [CrossRef]
17. Chaban Y, Boekema EJ, Dudkina NV. Structures of mitochondrial oxidative phosphorylation supercomplexes and mechanisms for their stabilisation. Biochim Biophys Acta. 2014; 1837: 418–426. [Medline] [CrossRef]
18. Kadenbach B, Hüttemann M. The subunit composition and function of mammalian cytochrome c oxidase. Mitochondrion. 2015; 24: 64–76. [Medline] [CrossRef]
19. Hüttemann M, Jaradat S, Grossman LI. Cytochrome c oxidase of mammals contains a testes-specific isoform of subunit VIb--the counterpart to testes-specific cytochrome c? Mol Reprod Dev. 2003; 66: 8–16. [Medline] [CrossRef]
20. Hüttemann M, Schmidt TR, Grossman LI. A third isoform of cytochrome c oxidase subunit VIII is present in mammals. Gene. 2003; 312: 95–102. [Medline] [CrossRef]
21. Akter MS, Hada M, Shikata D, Watanabe G, Ogura A, Matoba S. CRISPR/Cas9-based genetic screen of SCNT-reprogramming resistant genes identifies critical genes for male germ cell development in mice. Sci Rep. 2021; 11: 15438. [Medline] [CrossRef]
22. Hasuwa H, Muro Y, Ikawa M, Kato N, Tsujimoto Y, Okabe M. Transgenic mouse sperm that have green acrosome and red mitochondria allow visualization of sperm and their acrosome reaction in vivo. Exp Anim. 2010; 59: 105–107. [Medline] [CrossRef]
23. Miyata H, Oura S, Morohoshi A, Shimada K, Mashiko D,

Oyama Y, et al. SPATA33 localizes calcineurin to the mitochondria and regulates sperm motility in mice. Proc Natl Acad Sci USA. 2021; 118: e2106673118. [Medline] [CrossRef]
24. Abbasi F, Miyata H, Shimada K, Morohoshi A, Nozawa K, Matsumura T, et al. RSPH6A is required for sperm flagellum formation and male fertility in mice. J Cell Sci. 2018; 131: jcs221648. [Medline] [CrossRef]
25. Toyoda Y, Yokoyama M. The Early History of the TYH medium for in vitro fertilization of mouse ova. J Mamm Ova Res. 2016; 33: 3–10. [CrossRef]
26. Lawitts JA, Biggers JD. Culture of preimplantation embryos. Methods Enzymol. 1993; 225: 153–164. [Medline] [CrossRef]
27. Dranka BP, Hill BG, Darley-Usmar VM. Mitochondrial reserve capacity in endothelial cells: The impact of nitric oxide and reactive oxygen species. Free Radic Biol Med. 2010; 48: 905–914. [Medline] [CrossRef]
28. Miyata H, Satouh Y, Mashiko D, Muto M, Nozawa K, Shiba K, et al. Sperm calcineurin inhibition prevents mouse fertility with implications for male contraceptive. Science. 2015; 350: 442–445. [Medline] [CrossRef]
29. Baba SA, Mogami Y. An approach to digital image analysis of bending shapes of eukaryotic flagella and cilia. Cell Motil. 1985; 5: 475–489. [CrossRef]
30. Miyata H, Shimada K, Morohoshi A, Oura S, Matsumura T, Xu Z, et al. Testis-enriched kinesin KIF9 is important for progressive motility in mouse spermatozoa. FASEB J. 2020; 34: 5389–5400. [Medline] [CrossRef]
31. Hallmann K, Kudin AP, Zsurka G, Kornblum C, Reimann J, Stüve B, et al. Loss of the smallest subunit of cytochrome c oxidase, COX8A, causes Leigh-like syndrome and epilepsy. Brain. 2016; 139: 338–345. [Medline] [CrossRef]
32. Robertson MJ, Kent K, Tharp N, Nozawa K, Dean L, Mathew M, et al. Large-scale discovery of male reproductive tract-specific genes through analysis of RNA-seq datasets. BMC Biol. 2020; 18: 103. [Medline] [CrossRef]
33. Soto IC, Fontanesi F, Liu J, Barrientos A. Biogenesis and assembly of eukaryotic cytochrome c oxidase catalytic core. Biochim Biophys Acta. 2012; 1817: 883–897. [Medline] [CrossRef]
34. Helling S, Hüttemann M, Ramzan R, Kim SH, Lee I, Müller T, et al. Multiple phosphorylations of cytochrome c oxidase and their functions. Proteomics. 2012; 12: 950–959. [Medline] [CrossRef]
35. Muller B, Lewis N, Adeniyi T, Leese HJ, Brison DR, Sturmey RG. Application of extracellular flux analysis for determining mitochondrial function in mammalian oocytes and early embryos. Sci Rep. 2019; 9: 16778. [Medline] [CrossRef]
36. Visconti PE, Bailey JL, Moore GD, Pan D, Olds-Clarke P, Kopf GS. Capacitation of mouse spermatozoa. I. Correlation between the capacitation state and protein tyrosine phosphorylation. Development. 1995; 121: 1129–1137. [Medline] [CrossRef]
37. Cheng CC, Wooten J, Gibbs ZA, McGlynn K, Mishra P, Whitehurst AW. Sperm-specific COX6B2 enhances oxidative phosphorylation, proliferation, and survival in human lung adenocarcinoma. eLife. 2020; 9: e58108. [Medline] [CrossRef]
38. Nie K, Li J, He X, Wang Y, Zhao Q, Du M, et al. COX6B2 drives metabolic reprogramming toward oxidative phosphorylation to promote metastasis in pancreatic ductal cancer cells. Oncogenesis. 2020; 9: 51. [Medline] [CrossRef]